Mineral Aerosol Phenomena on Mars: Implications for Atmospheric Dynamics

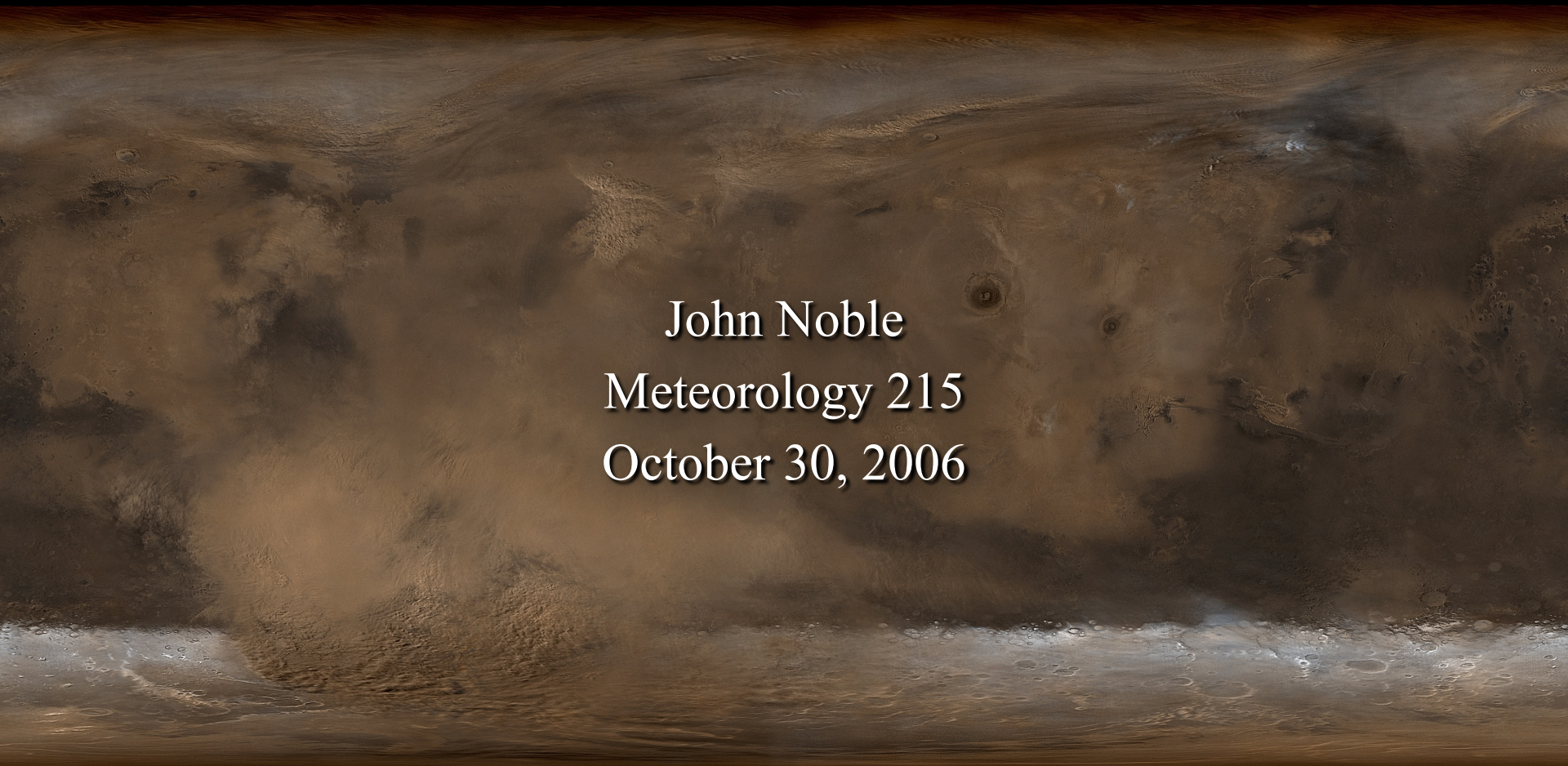

John Noble

Meteorology 215

October 30, 2006

Outline

October 30

- Introduction
- Overview of Mars
  - Geology
  - Climate
  - Weather
  - Aerosols
    - Properties
    - Phenomena
    - Impacts

November 1

- Comparative overview of Earth and Mars
  - Geology
  - Climate
  - Weather
  - Aerosols
    - Properties
    - Phenomena
    - Impacts

Introduction to Mars

- Fourth terrestrial planet from the Sun
- Closest to Earth in many respects
  - Radiative environment
  - Length off the solar day
  - Axis tilt
  - Geophysical systems:
    - Atmosphere
    - Cryosphere
    - Lithosphere
    - Hydrosphere (possibly in Martian history)

Earth Mars comparison

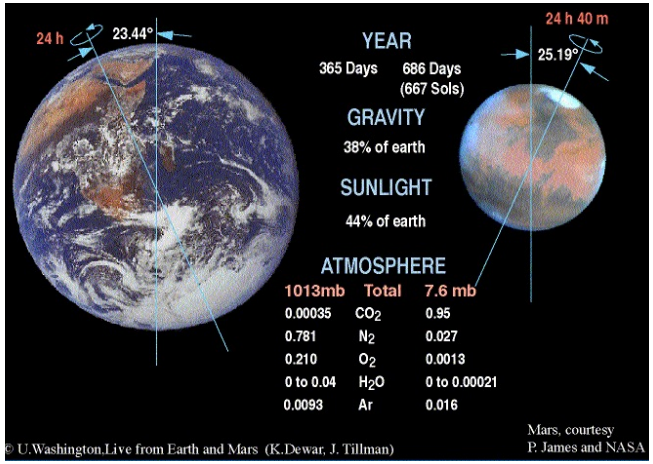

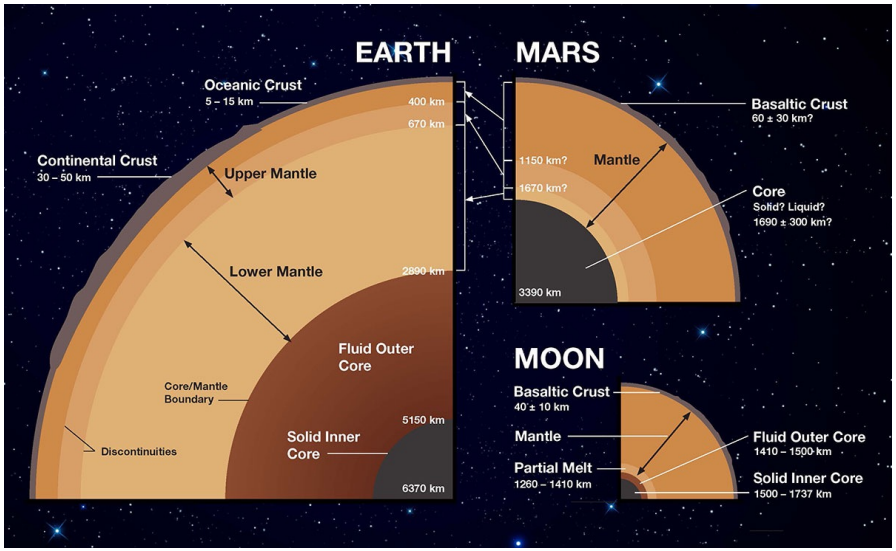

Planetary & atmospheric parameters for Mars and Earth

Parameter	Mars	Earth
Mass (kg)	6.46×10^{23}	5.98×10^{24}
Semi-major axis, ($\times 10^6$ km) (AU)	227.9 1.52	149.6 1.0
Orbital eccentricity	0.093	0.017
Planetary obliquity (°)	25.19	23.93
Rotation rate, $\Omega\left(10^{-5} \cdot \mathrm{s}^{-1}\right)$	7.088	7.294
Solar day (s)	88,775	86,400
Year length (Earth days)	686.98	365.24
Equatorial radius, r_{eq} (km)	3,394	6,369
Surface gravity, $g\left(\mathrm{m} \cdot \mathrm{s}^{-2}\right)$	3.72	9.81
Surface air pressure, p (hPa)	6.1*	1013
Constituents of lower (<120 km) atmosphere (molar ratio, %)	CO_2 (95) N_2 (2.7) ^{40}Ar (1.6) O_2 (0.13) H_2O (0.03)*	CO_2 (0.037) N_2 (77) ^{40}Ar (0.9) O_2 (21) H_2O (0–4)
Solar flux ("solar constant"), S_0 $\left(\mathrm{W} \cdot \mathrm{m}^{-2}\right)$	589	1367
Radiative equilibrium temperature, $T_e\left(\mathrm{K}\right)$	210	256
Scale height, $H_p = \dfrac{RT_e}{g}\left(\mathrm{km}\right)$	10.8	7.5
Gas constant, $R\left(\mathrm{J} \cdot \mathrm{kg}^{-1} \cdot \mathrm{K}^{-1}\right)$	192	287
Specific heat at constant pressure, $c_p\left(\mathrm{J} \cdot \mathrm{kg}^{-1} \cdot \mathrm{K}^{-1}\right)$	831	1000
Dry adiabatic lapse rate, $\Gamma_d\left(\mathrm{K} \cdot \mathrm{km}^{-1}\right)$	4.5	9.8
Mean lapse rate of lowest scale height, Γ ($\mathrm{K\ km^{-1}}$)	2.5	6.5
Buoyancy (Brunt–Väisälä) frequency, N ($10^{-2}\ \mathrm{s}^{-1}$)	~0.6	1.12
Bulk radiative timescale, τ_r (10^5 s)	2	40
Typical zonal wind at jet level, $U\left(\mathrm{m} \cdot \mathrm{s}^{-1}\right)$	80	30

* Variable with season. $\bar{p} \approx 6.1$ hPa. Spatial and temporal range ≈ 4–10 hPa

(Haberle 2003; Leovy 2001; Owen 1992; Read and Lewis 2004; Zurek *et al.* 1992)

Surface pressure

- 1–9 hPa (mean ≈ 6 hPa)
- Function of season and altitude

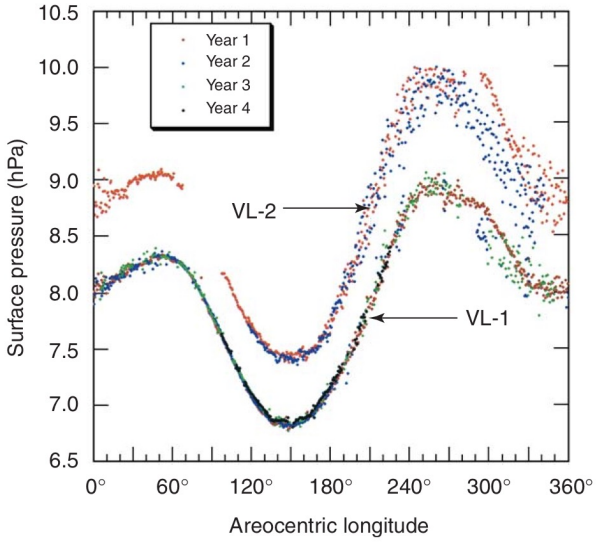

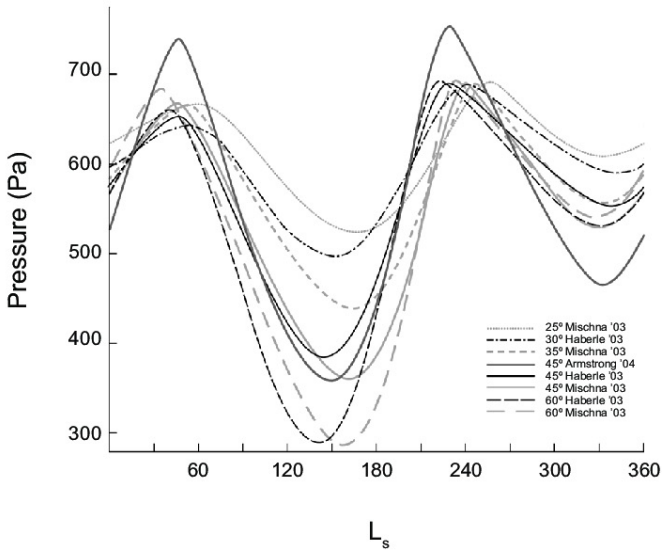

Figure 5 Seasonal variation of the daily averaged surface pressure on Mars measured by the *Viking Landers*.

(Haberle 2003)

Atmospheric constituents

Composition

95.32%	Carbon dioxide
2.7%	Nitrogen
1.6%	Argon
0.13%	Oxygen
0.07%	Carbon monoxide
0.03%	Water vapor
Trace:	Neon, krypton, xenon, ozone, methane

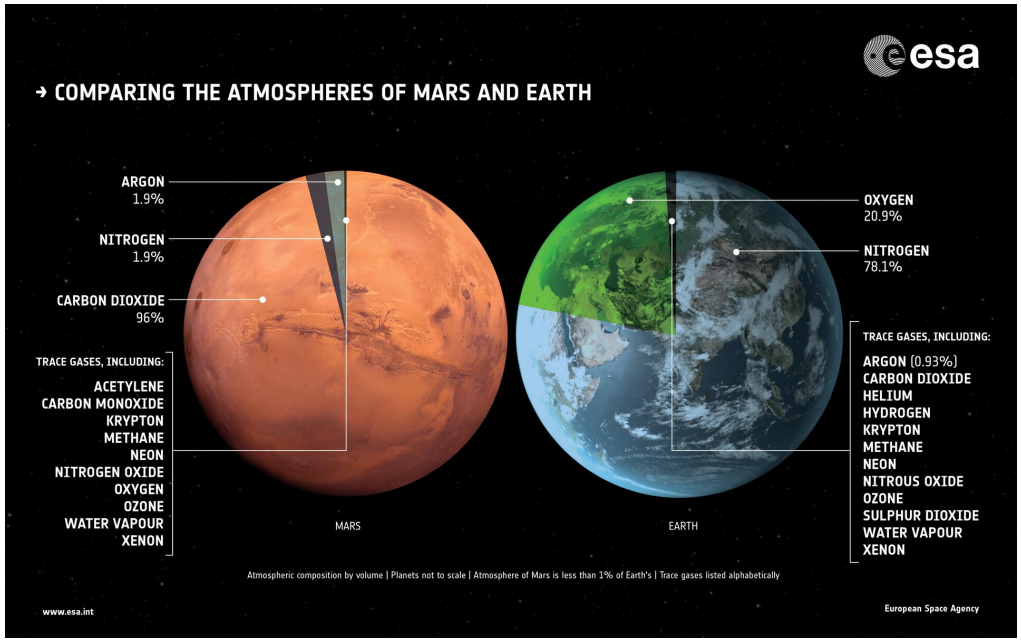

Time

- The fundamental unit of time is the SI second.
- The Martian day is known as ‘sol’, and consists of 88,775 seconds.
- Each sol is divided into 24 Martian hours, which are equivalent to 24.63 Earth hours.
- Seasons are measured in degrees of aerocentric longitude, L_s, which is an angular measure of the Sun relative to Mars. The spring equinox in the Northern Hemisphere (NH) occurs at L_s=0º, NH summer solstice at L_s=90º, NH fall equinox at L_s=180º, and winter solstice at L_s=270º.
- The seasons are reversed for the Southern Hemisphere (SH), as they are on Earth, and thus SH spring equinox occurs at L_s=180º.

Time

- The Martian year consists of 686.98 sols, and is measured in Mars years (MY) that begin on L_s=180º, MY1.
- This corresponds to April 11, 1955, and was chosen because of global dust storm observations that Mars year.
- The best documented planet-encircling dust event (PDE), occurred at L_s=180º, MY25 (June to November, 2001).

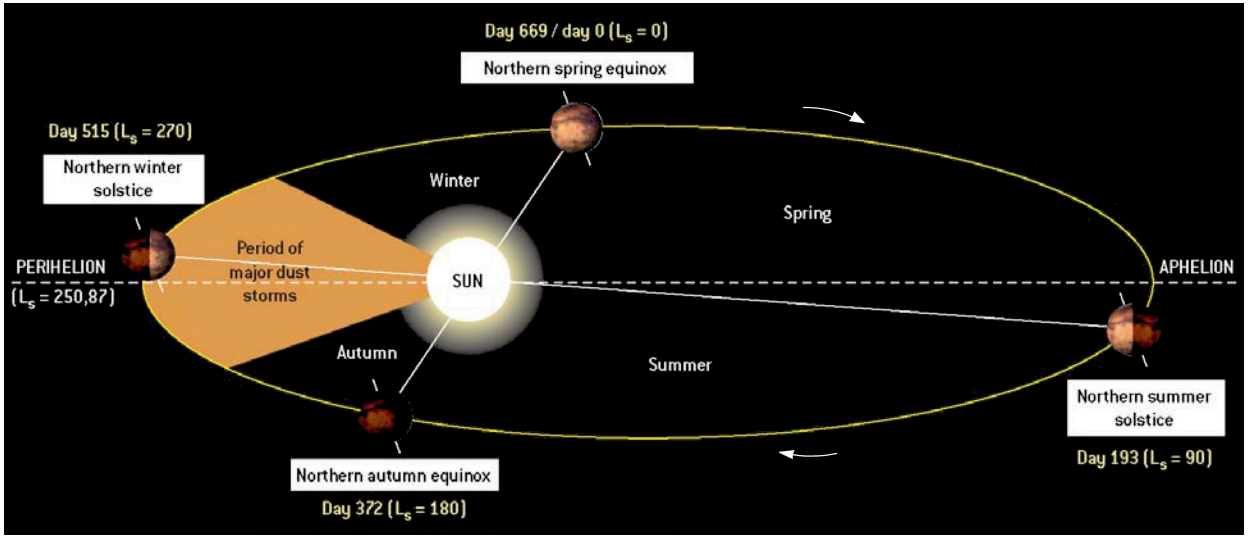

Martian orbit and seasons

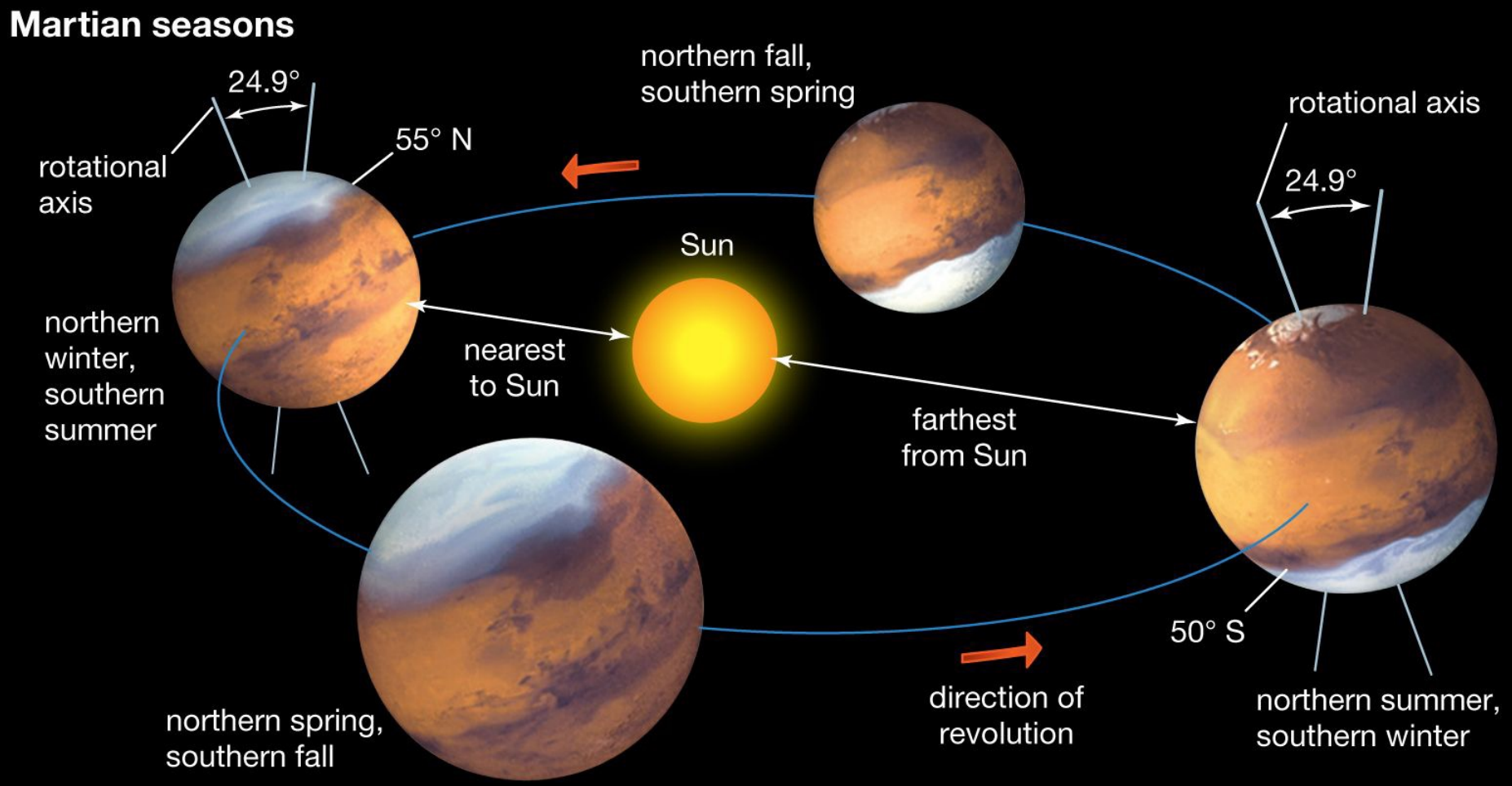

Comparison of the atmospheres of Mars & Earth

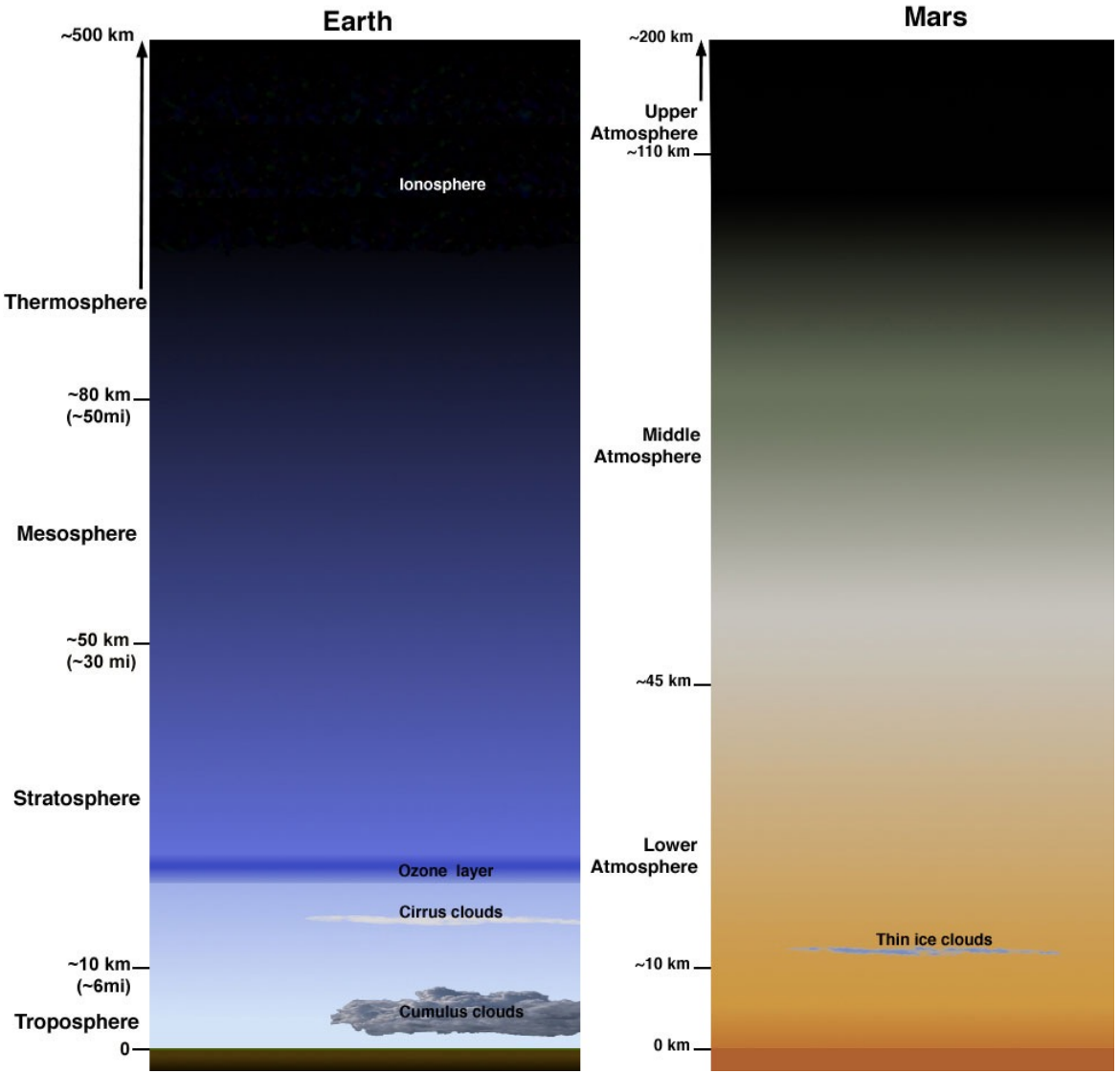

Vertical structure of the Martian atmosphere

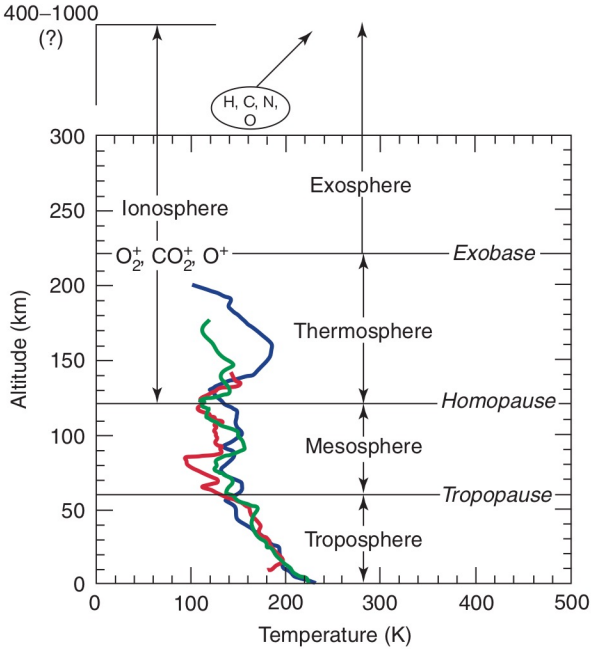

Figure 1 Vertical structure of the Martian atmosphere. Colored curves are temperatures inferred from deceleration measurements aboard the *Viking 1* (blue), *Viking 2* (green), and *Pathfinder* (red) landers.

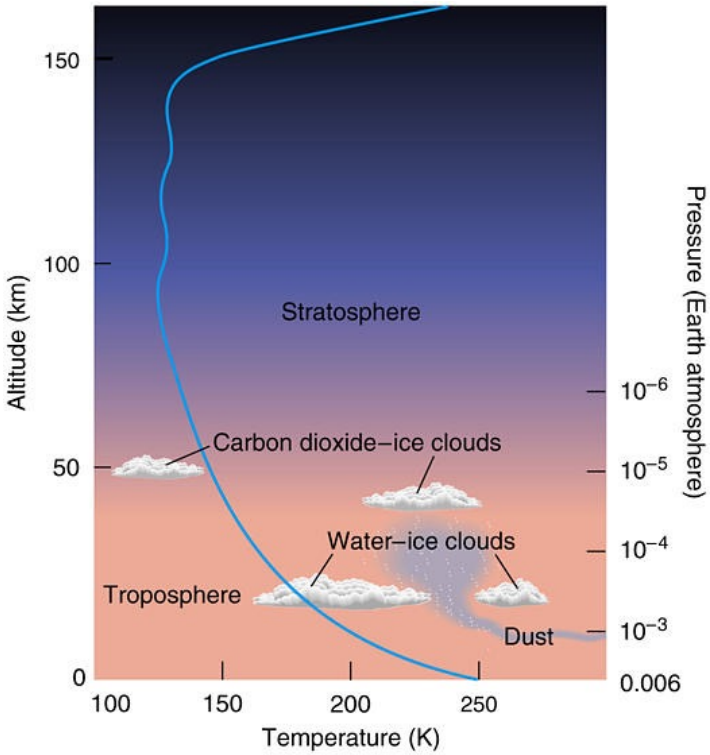

(Haberle 2003)

General circulation & atmospheric processes

General circulation of the lower atmosphere at (a) equinoxes, and (b) solstices (Haberle 1997). (c) Atmospheric processes (Haberle 2003)

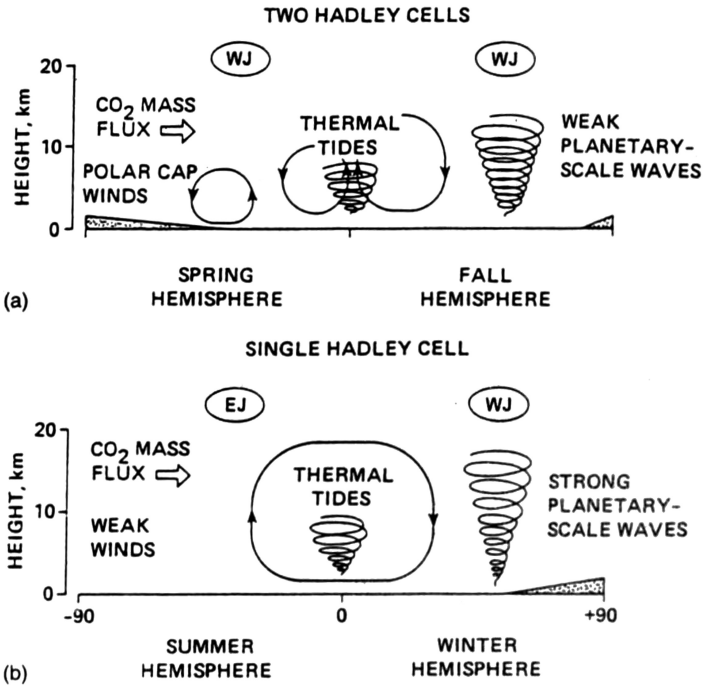

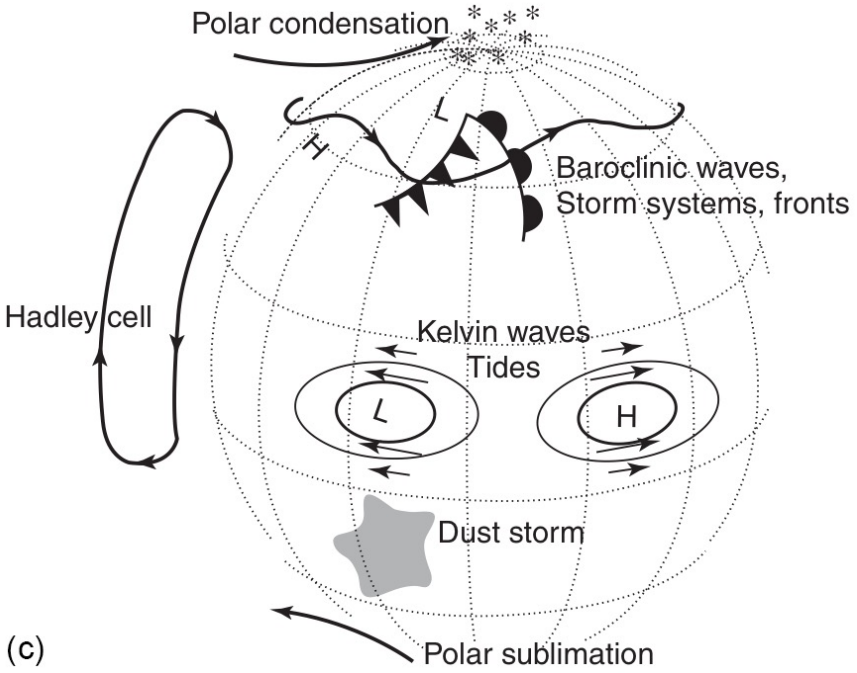

Blackbody emission & temperature

- Surface temperatures range from 150 K to 275 K.
- Although the Martian atmosphere is composed primarily of CO_2 (95%), greenhouse warming raises temperatures by only 5 K above the radiative equilibrium temperature.
- The atmosphere only absorbs radiation in a narrow band of the spectrum.
- 40% seasonal change in insolation, compared with 6% for Earth.

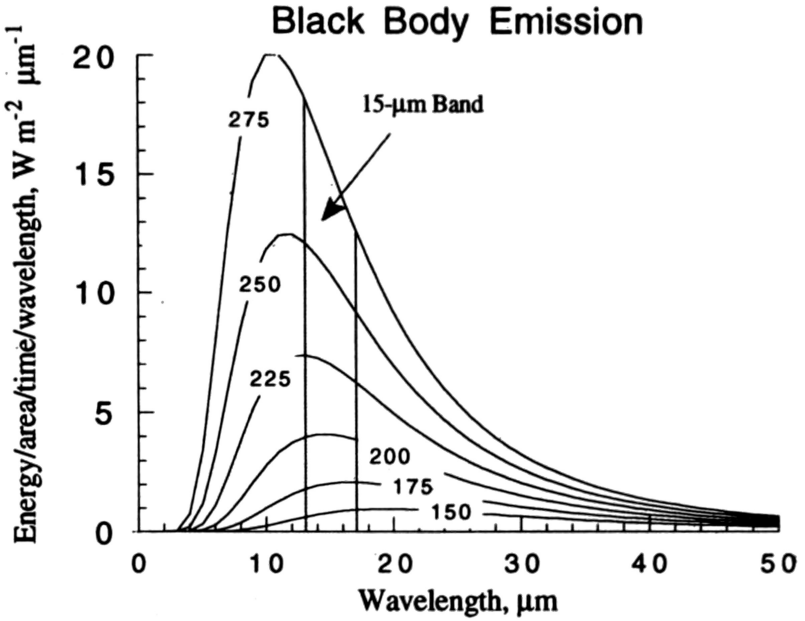

Figure M24 Blackbody emission as a function of wavelength for a range of temperatures representative of the Martian surface. CO_2 is the principal infrared absorbing gas in the Martian atmosphere and the approximate width of its 15-μm absorption feature is indicated.

(Haberle 1997)

Greenhouse effect

$$T_e = \left(\frac{S_0 \left(1 - A_p\right)}{4\sigma} \right)^{1/4}$$

T_e = Effective Temperature = 210 K

T_s = Average Surface Temp = 215 K

A_p = Planetary Albedo = 0.26

S_0 = Solar Flux = 590 W m^{-2}

σ = Stefan-Boltzman Constant

$$T_s - T_e = 5 \text{ K}$$

Topography

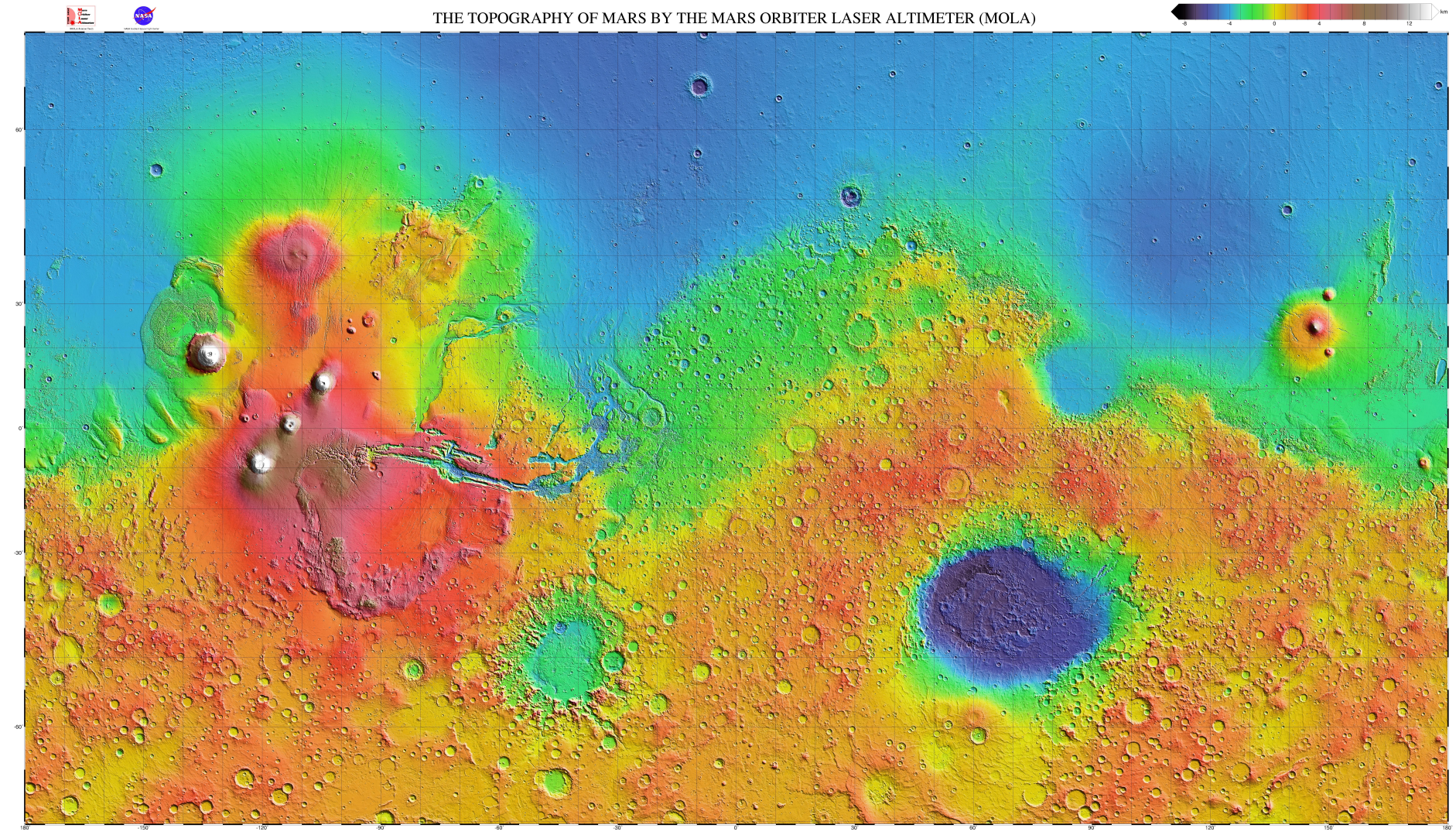
THE TOPOGRAPHY OF MARS BY THE MARS ORBITER LASER ALTIMETER (MOLA)
km
-8
-4
0
4
8
12
60
30
0
-30
-60
180
-150
-120
-90
-60
-30
0
30
60
90
120
150
180

History

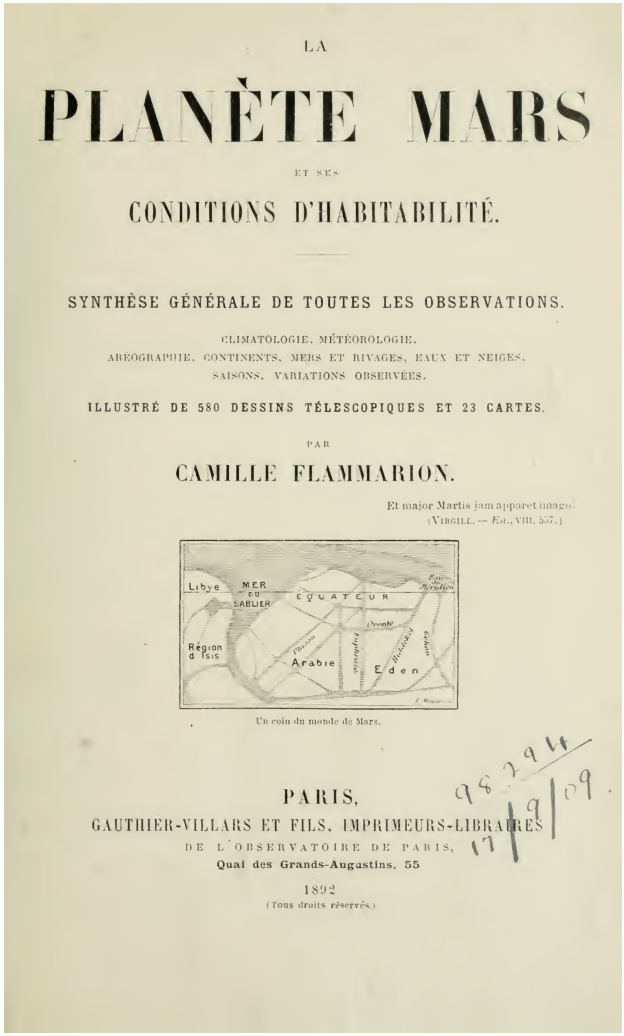

LA

PLANÈTE MARS

ET SES

CONDITIONS D'HABITABILITÉ.

SYNTHÈSE GÉNÉRALE DE TOUTES LES OBSERVATIONS.

CLIMATOLOGIE. MÉTÉOROLOGIE.
ARÉOGRAPHIE. CONTINENTS, MERS ET RIVAGES, EAUX ET NEIGES.
SAISONS. VARIATIONS OBSERVÉES.

ILLUSTRÉ DE 580 DESSINS TÉLESCOPIQUES ET 23 CARTES.

PAR

CAMILLE FLAMMARION.

Et major Martis jam apparet imago.
(VIRGILE. — *Én.*, VIII, 557.)

Un coin du monde de Mars.

PARIS,
GAUTHIER-VILLARS ET FILS, IMPRIMEURS-LIBRAIRES
DE L'OBSERVATOIRE DE PARIS,
Quai des Grands-Augustins, 55

1892

(Tous droits réservés.)

Yellow-colored regions ("yellow clouds") have been observed for ~ two centuries, first by Flaugergues in the late 1700s and early 1800s (Flammarion 1892), and later by Schiaparelli (1893b, 1899), Flammarion (1892), and others.

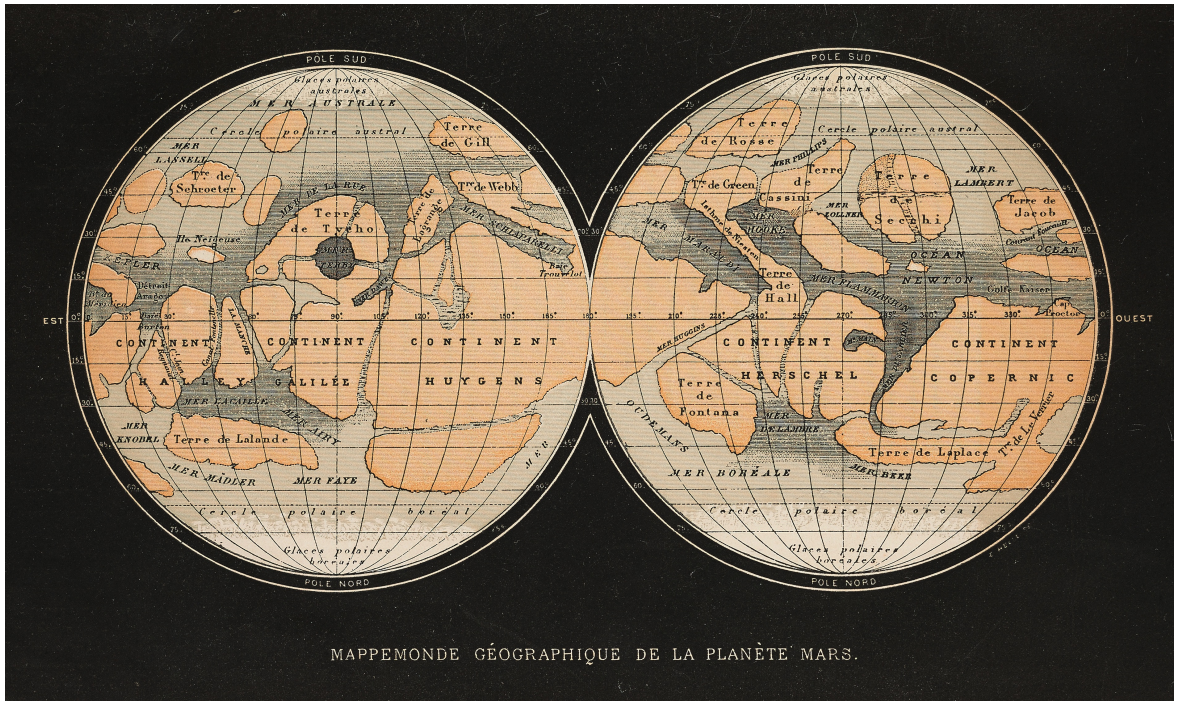

MAPPEMONDE GÉOGRAPHIQUE DE LA PLANÈTE MARS.

(Flammarion 1892)

Mineral aerosols

- Dynamically, radiatively, and thermally coupled with the atmosphere
- Influence weather, climate, and atmospheric circulation
- Agents of geological change
- Absorb and scatter incoming solar radiation
- Absorb and emit IR radiation
- Dust optical depth has large variability

$$\sigma_\lambda = \sec\theta \, k_\lambda \int_0^x \rho \, dz$$

Mineral aerosols

- Composition:
  - 25% montmorillonite
  - 75% basalt

- IR radiation emitted from the aerosols is absorbed and re-emitted by CO_2, which in turn causes warming.

- Regional and global dust storms change the thermal structure of the atmosphere by:
  - lowering temperatures near the surface due to absorption of incoming solar radiation.
  - raising temperatures aloft.

- This subsequently affects the pressure, winds, and ultimately general circulation.

Thermal Emission Spectrometer (TES)

- TES is an interferometric spectrometer on the Mars Global Surveyor that measures thermal emission in the IR spectrum from 6–50 μm (wavenumbers 1600–200 cm^{-1}).
- There are six detectors yielding a spatial resolution of ~3 x 9 km on the surface (Smith *et al.* 2002).
- Spectral data are used to retrieve the following quantities:
  - temperature (surface and atmospheric)
  - optical depth (dust and water ice aerosol)
  - water vapor column abundance (Smith *et al.* 2000)
- Atmospheric thermal retrievals were obtained from 3.7–0.01 hPa, approximately 5.4–70.4 km.

We refer to 9-μm (IR) dust optical depth hereafter as 'opacity' (τ_d). All opacity retrievals have been normalized to remove the effects of topography.

Mars Global Surveyor

Thermal Emission Spectrometer (TES)

Radiance $I(\mu,\nu)$ measured by TES at the top of the atmosphere is formulated as

$$I(\mu,\nu) = \varepsilon(\nu)B(\nu,T_s)Tr(\mu,\nu,z_s) + \int_{z_s}^{z_t} B[\nu,T(z)]\frac{\partial Tr(\mu,\nu,z)}{\partial z}dz$$

After an atmospheric temperature retrieval has been calculated, an opacity retrieval is calculated with the following radiative transfer equation:

$$I_{\text{comp}}(\nu) = \varepsilon(\nu)B[T_{\text{surf}},\nu]e^{-\tau_0(\nu)/\mu} + \int_0^{\tau_0(\nu)} B[T(\tau),\nu]\, e^{-\tau/\mu}d\tau$$

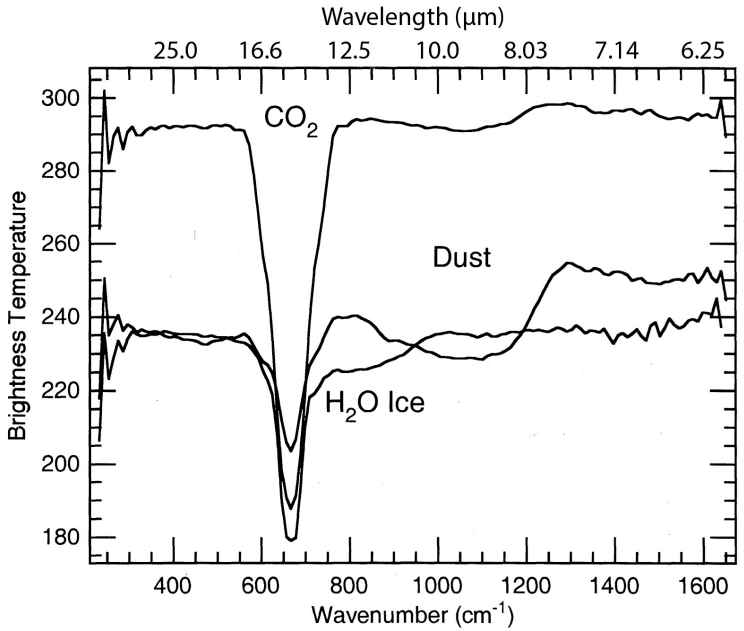

Daytime TES spectra (Smith *et al.* 2000)

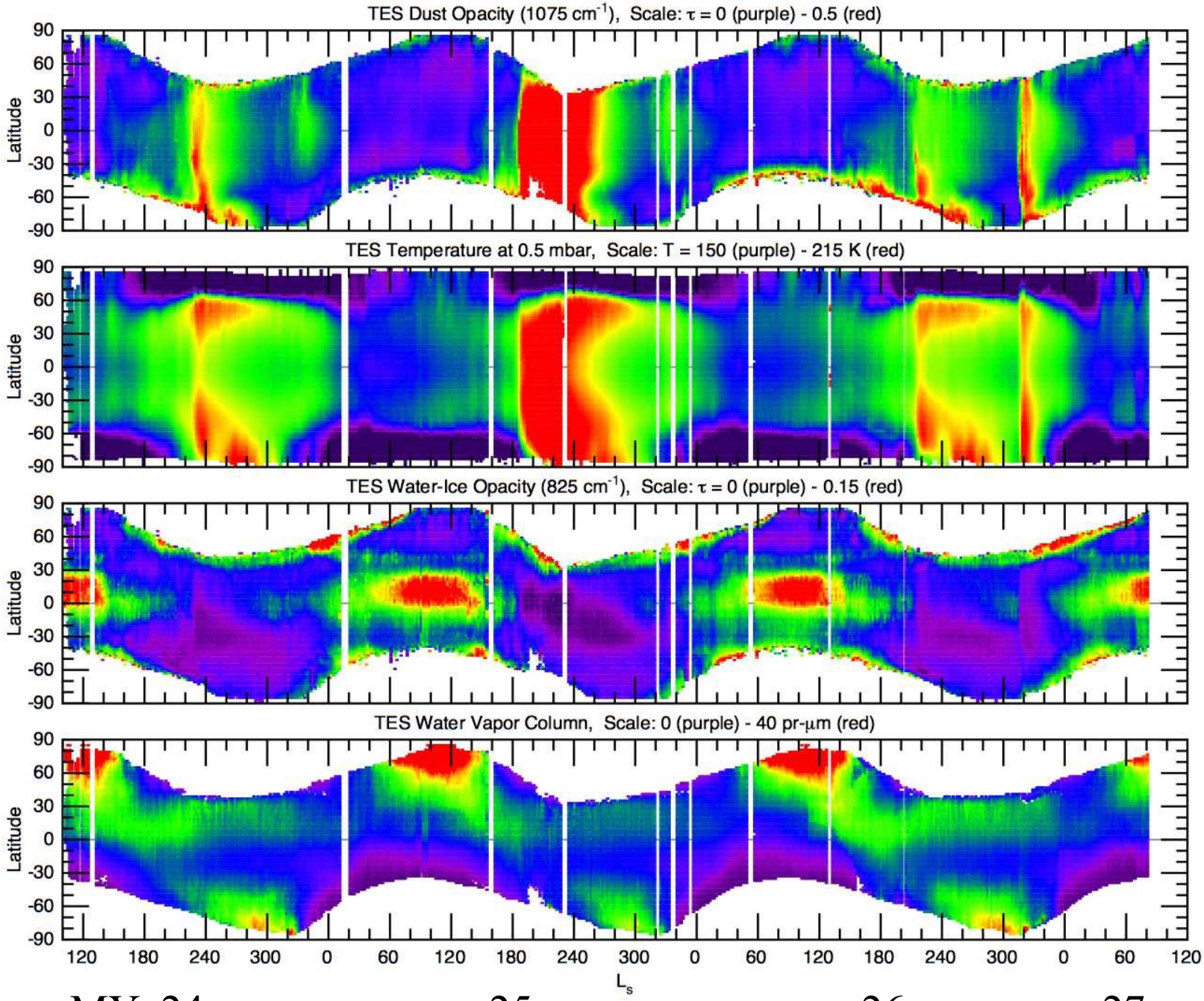
TES Dust Opacity (1075 cm^{-1}), Scale: τ = 0 (purple) - 0.5 (red)
TES Temperature at 0.5 mbar, Scale: T = 150 (purple) - 215 K (red)
TES Water-Ice Opacity (825 cm^{-1}), Scale: τ = 0 (purple) - 0.15 (red)
TES Water Vapor Column, Scale: 0 (purple) - 40 pr-μm (red)
Latitude
90
60
30
0
-30
-60
-90
120 180 240 300 0 60 120 180 240 300 0 60 120 180 240 300 0 60 120
L_s
MY 24
25
26
27

Planet-encircling dust events (PDE)

- Triggering mechanisms are not well understood. Theories involve feedbacks between heating and lifting.

- High amount of surface dust leads to dust storms
  - Common, but vary in size/strength
  - Range from local events (< 1km) – global events (> 5000 km)

- Dust lifted via dust devils or saltation
  - Driven by slope flow and strong daytime heating
  - Common in all seasons, although maximum activity occurs in the perihelion season (SH spring/summer)

- Activity most common near ice cap edges and large topographical features.

- Movement and redistribution of dust affects planetary and surface albedo.

MY 25 PDE

- The MY 25 PDE was documented by the Mars Global Surveyor (MGS) satellite
- The storm had a number of phases, including:
  - the initiation and early growth around the Hellas region
  - the development of new lifting centers downstream
  - the growth of the storm into global-scale
  - the decay phase

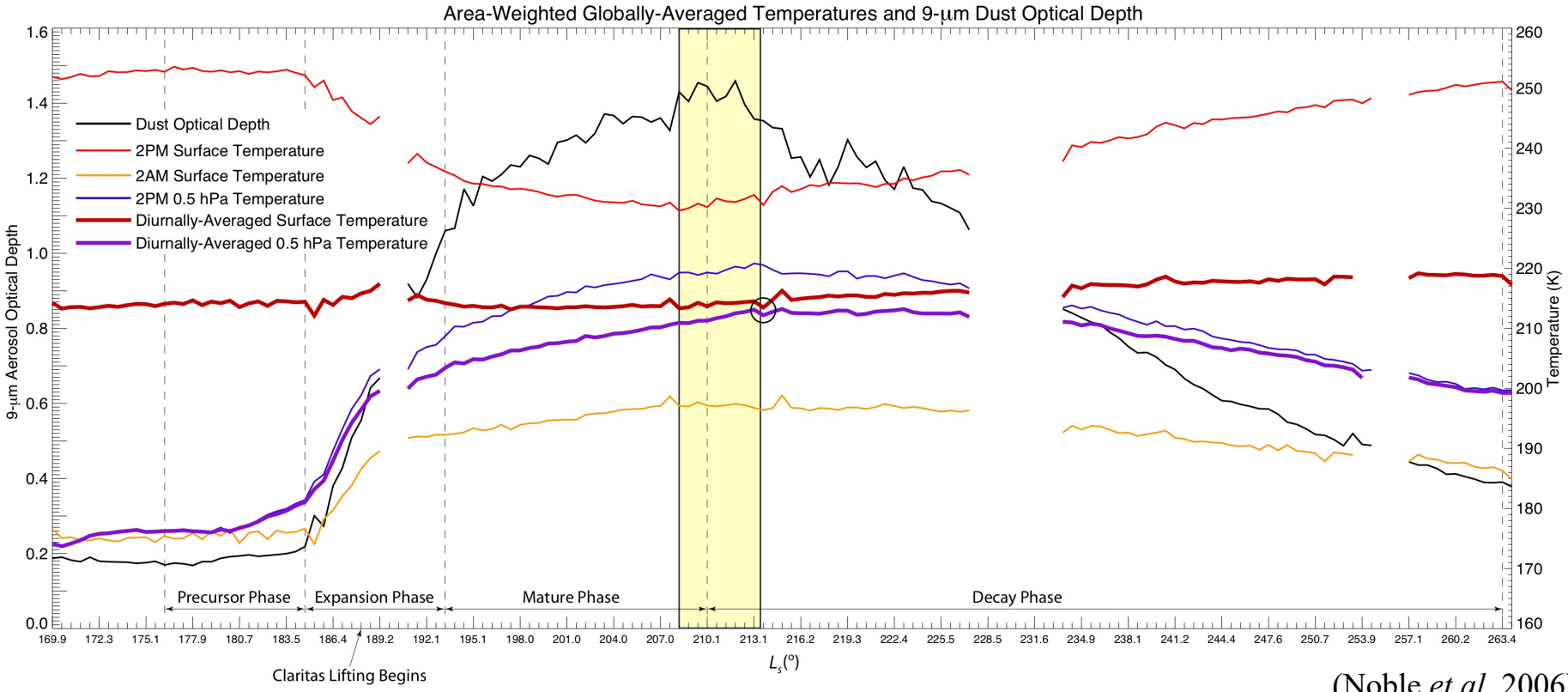

(Noble *et al.* 2006)

Storm onset in Hellas

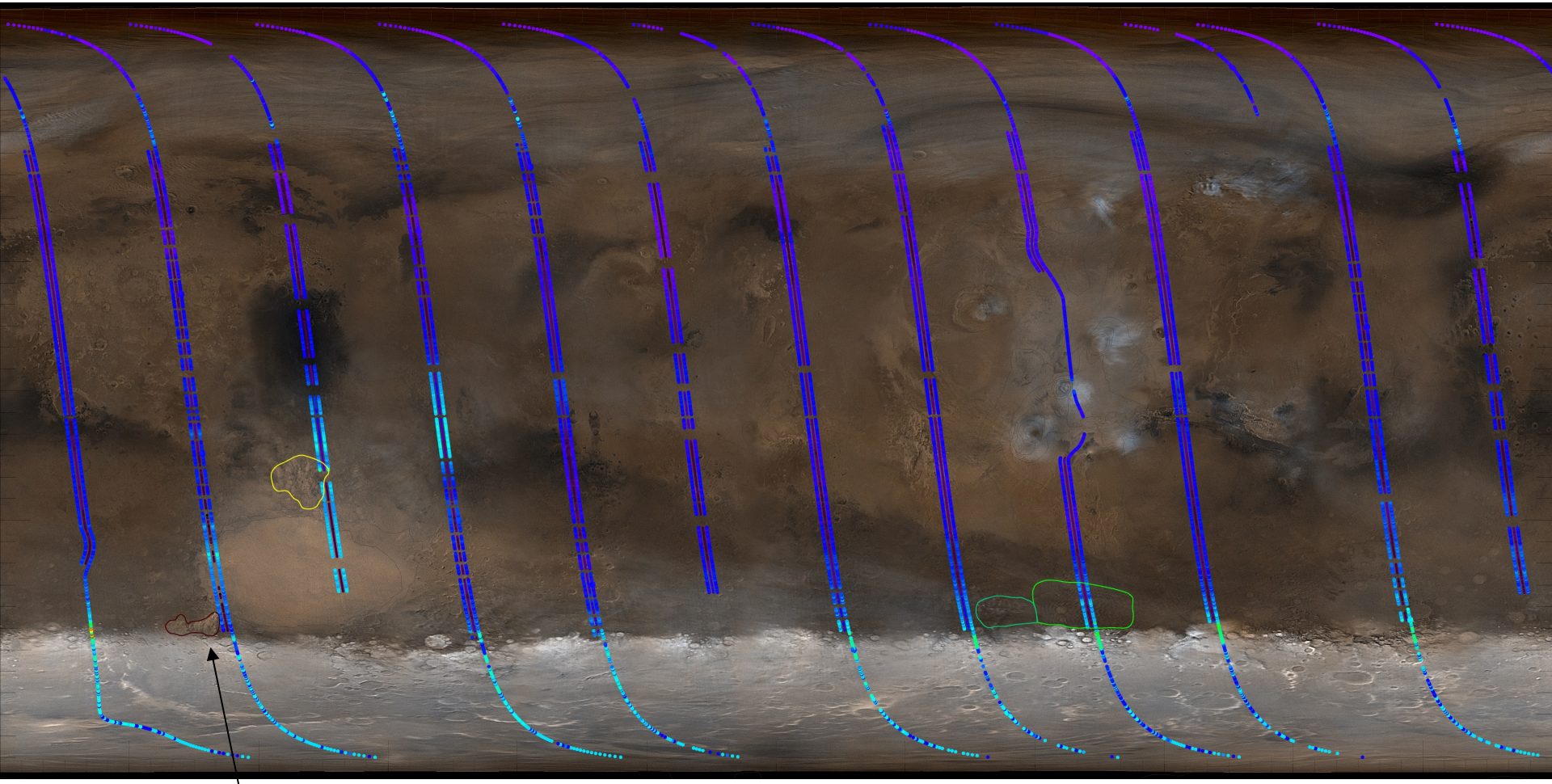

Pulse at L_s=181.8°

(Noble *et al.* 2006)

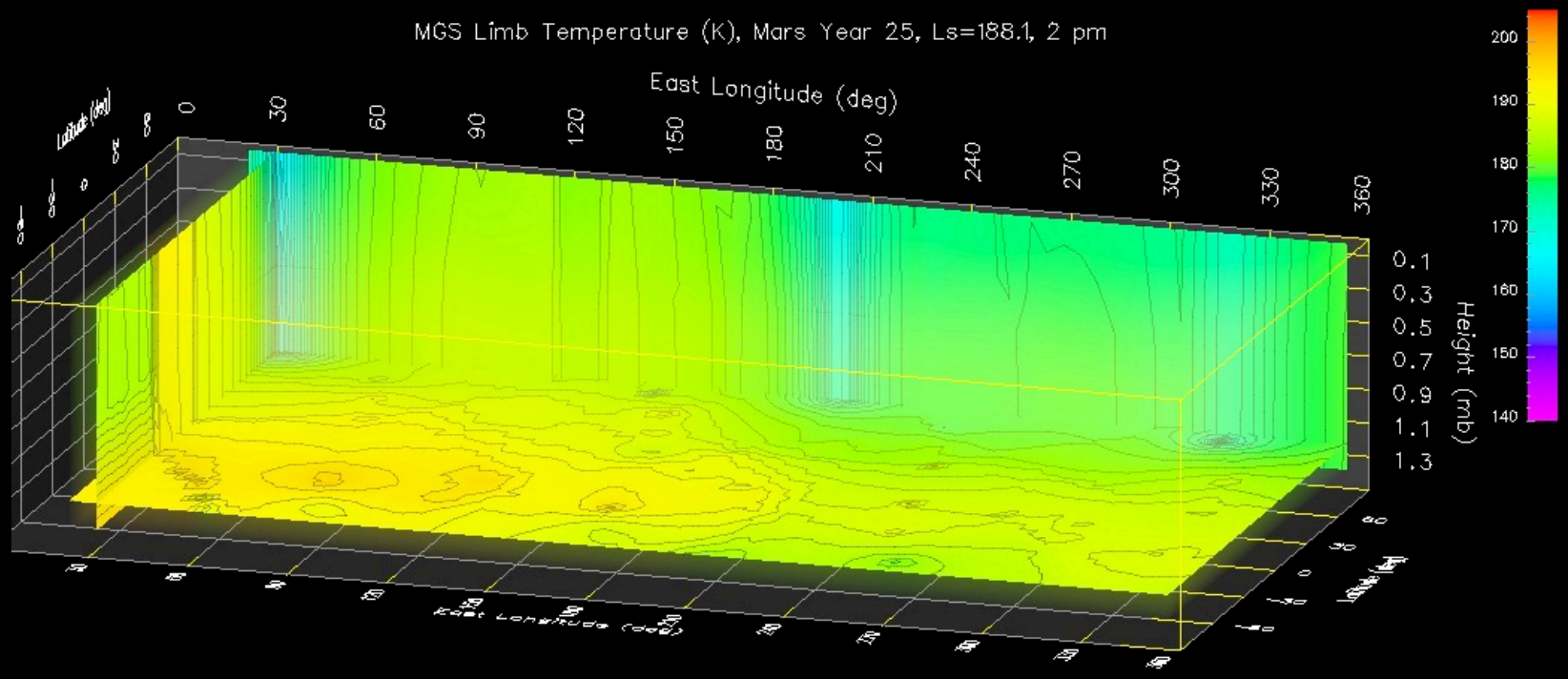
MGS Limb Temperature (K), Mars Year 25, Ls=188.1, 2 pm
East Longitude (deg)
0
30
60
90
120
150
180
210
240
270
300
330
360
0.1
0.3
0.5
0.7
0.9
1.1
1.3
Height (mb)
200
190
180
170
160
150
140

- TES data that has been filtered with Barnes' Fast Fourier Synoptic Map program show a sequence of cold centers from ~L_s= 175–182° in the Hellas region with an approximate 2-sol periodicity, confirming the presence of these eddies in the thermal field.

- This process removes the time-mean and the zonal mean along with the very low frequencies. The westward diurnal tide (wavenumber one) is also removed.

- We hypothesize that these eddies served to "prime the pump", leading to the regional-scale Hellas dust storm around L_s=184°.

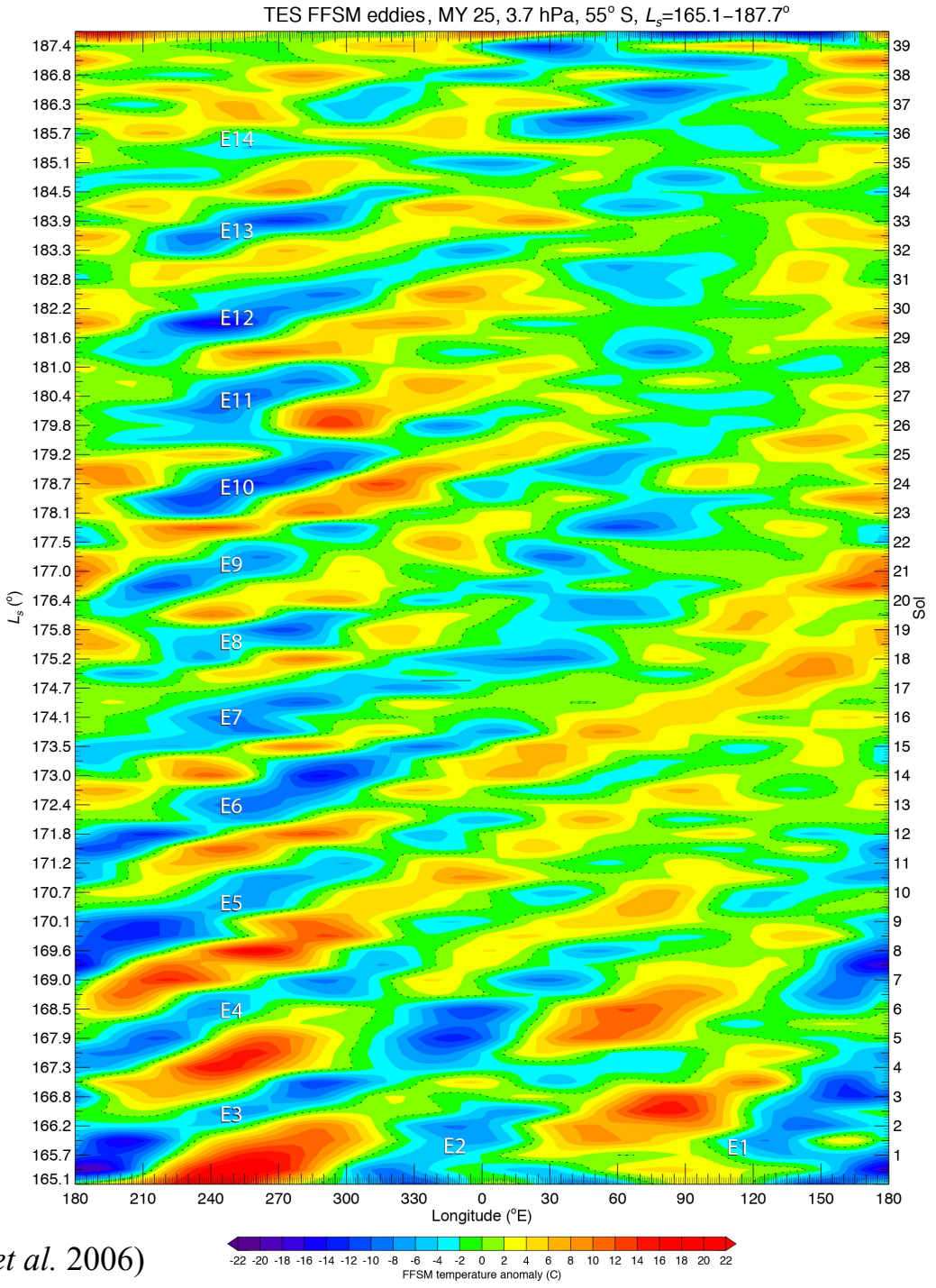

(Noble *et al.* 2006)

Wave one pattern

Both TES and MHSA data show the development of a wave one pattern with ridge in eastern hemisphere and trough in western hemisphere by L_s=181°, amplitude of ~5 K–10 K.

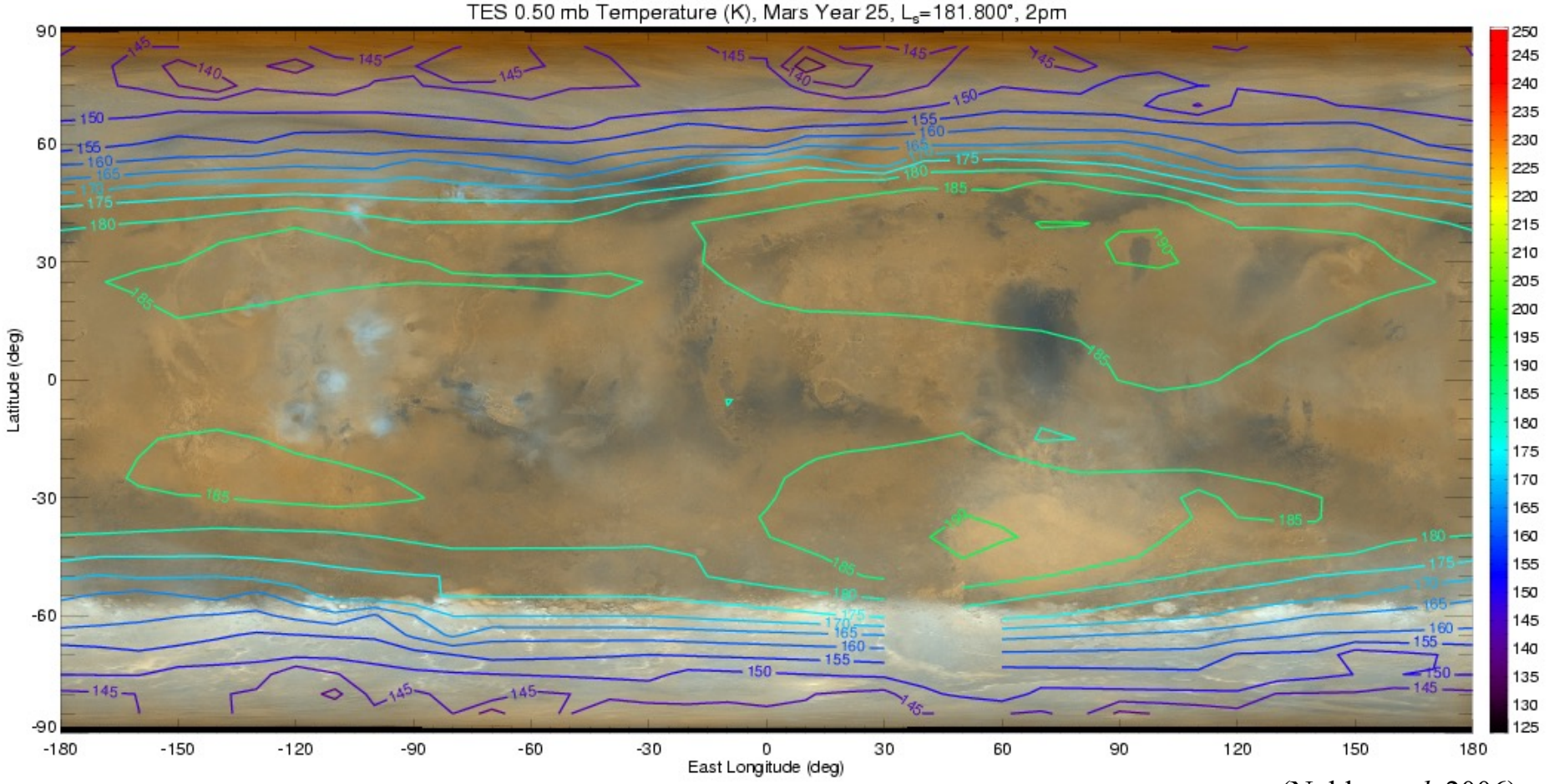

(Noble *et al.* 2006)

Expansion phase (L_s=184–205°)

MOC imagery with TES 2pm temperatures superimposed show that by L_s=187–188°, the lifted dust in the Hellas sector had led to the development of a large-amplitude quasi-stationary wave one feature in the temperature field from 0.11 hPa to 0.83 hPa, with a peak-to-trough amplitude of ~30 K (at 0.5 hPa).

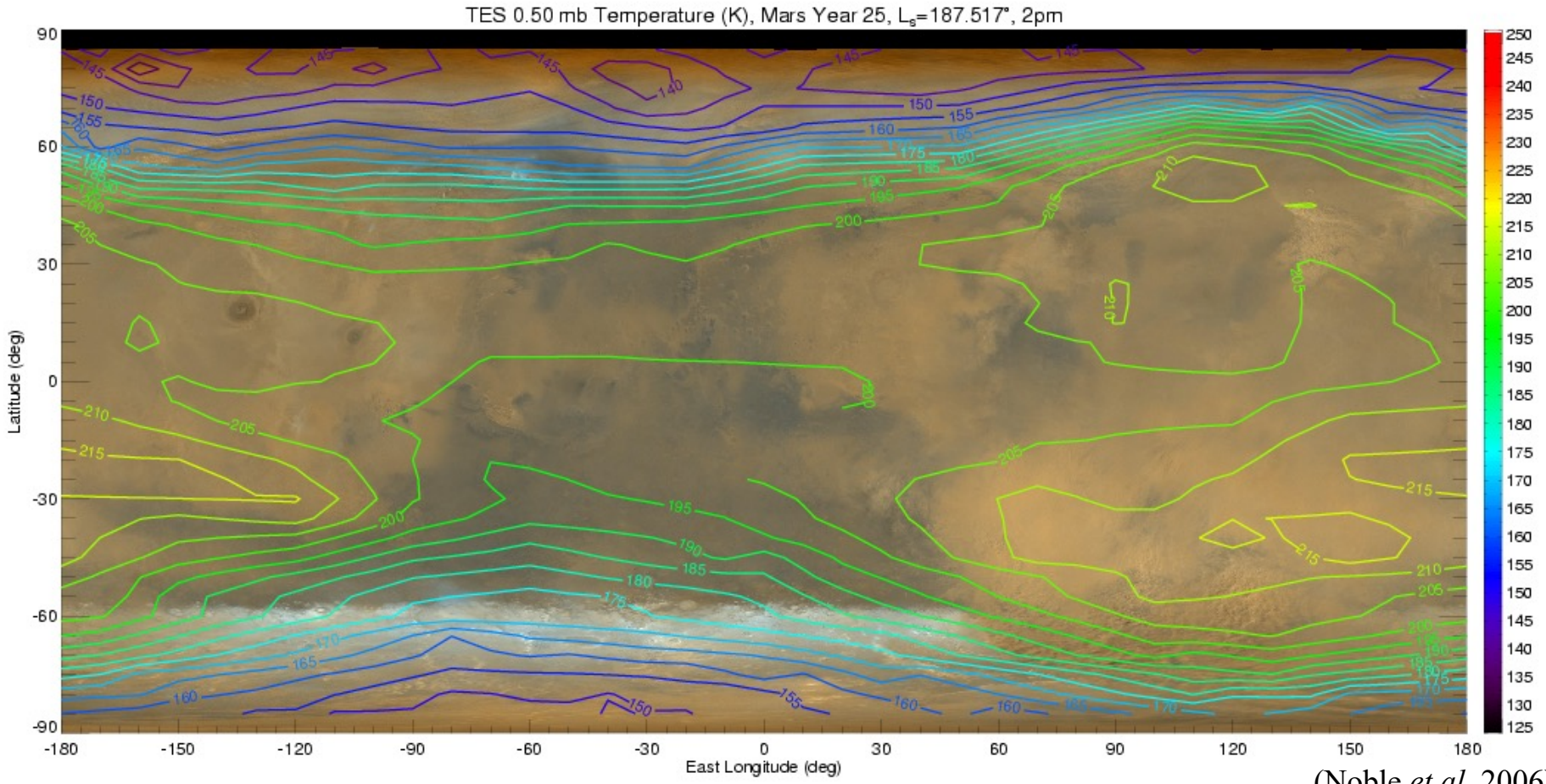

(Noble *et al.* 2006)

Second storm center develops in Claritas region

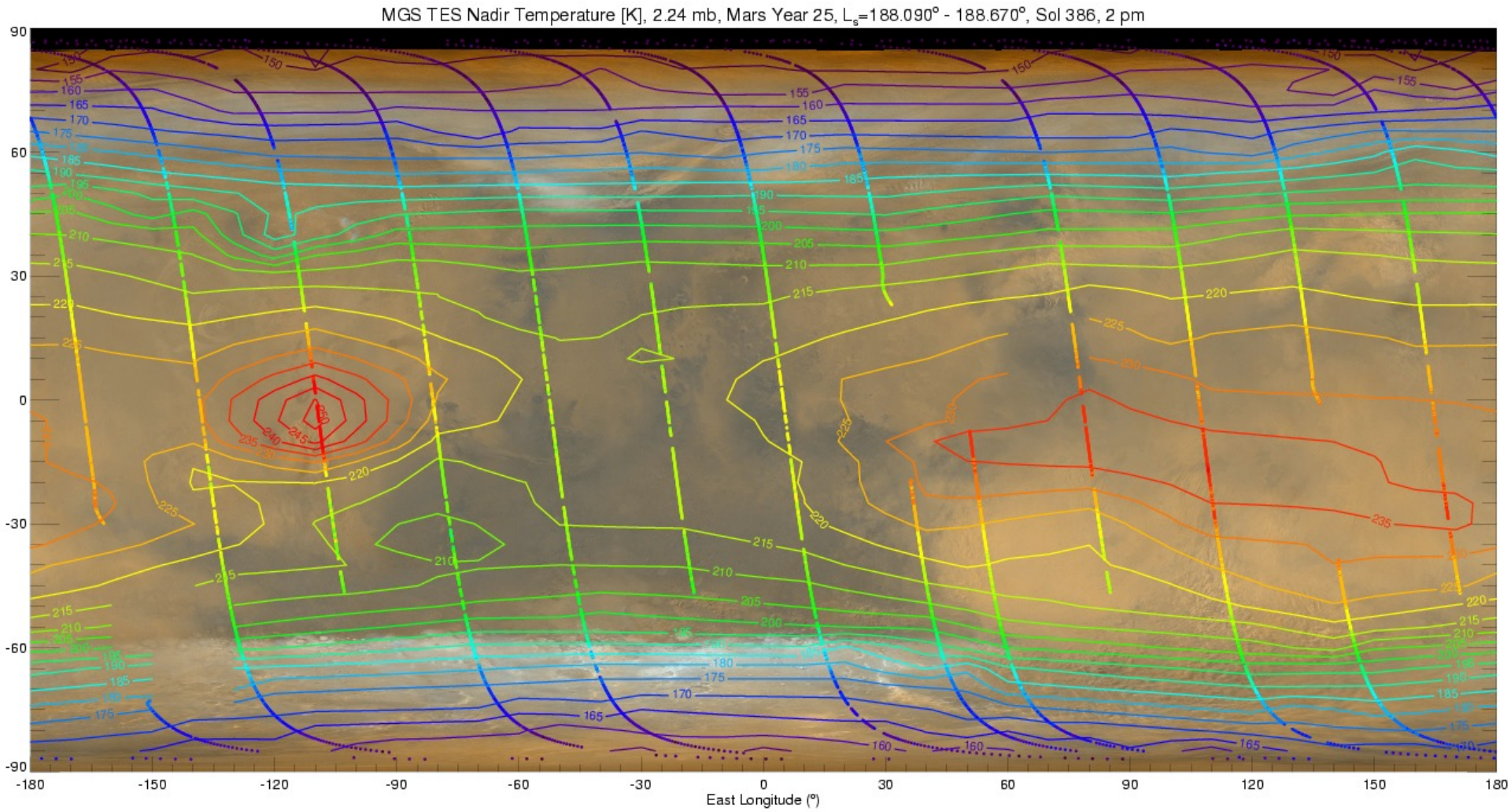

(Noble *et al.* 2006)

Second storm center develops in Claritas region

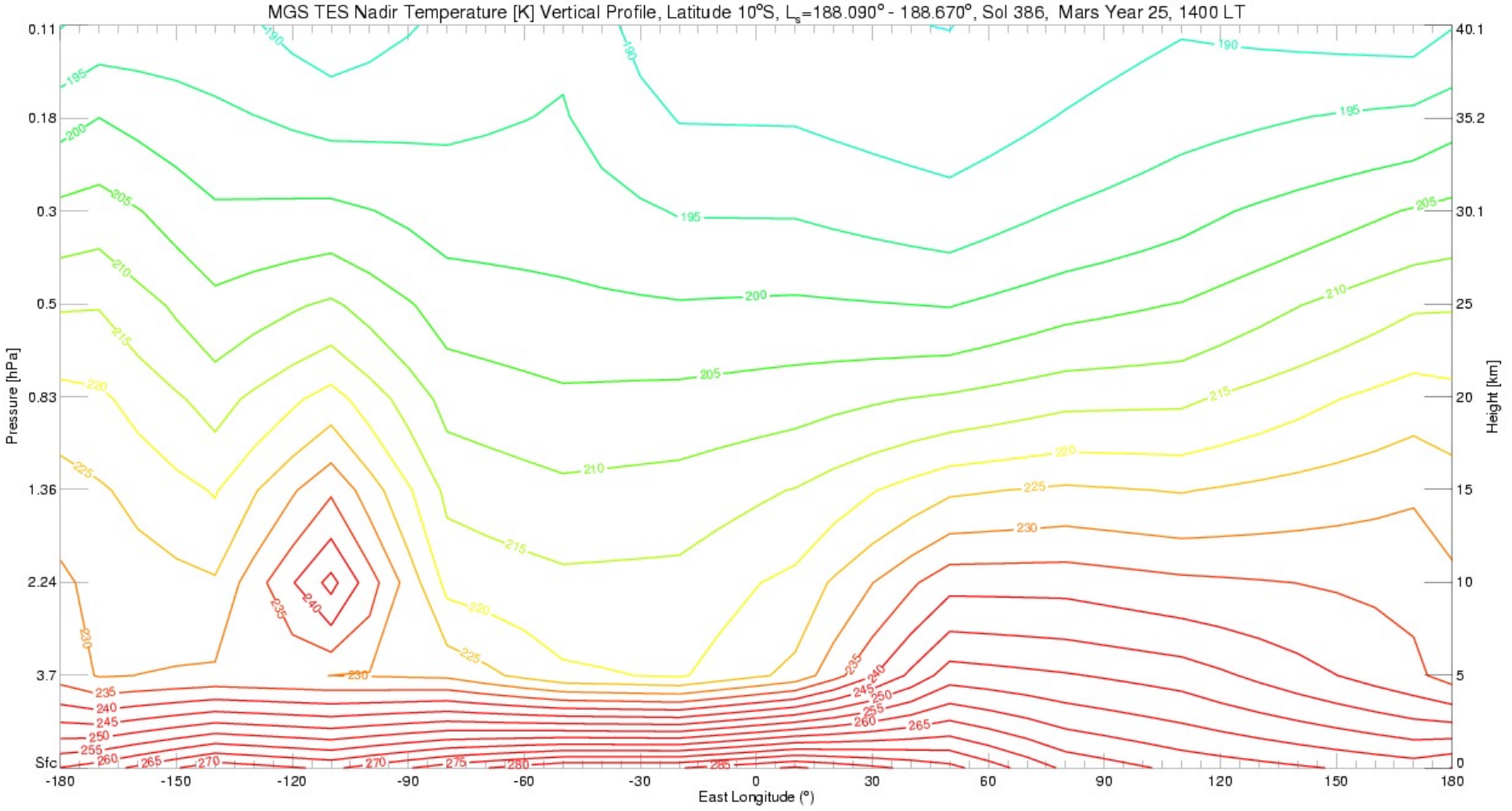

(Noble *et al.* 2006)

Thermal changes

- Globally-averaged daytime surface temperature decreased by 23 K at the height of the MY 25 PDE compared to the previous Martian year.
- Nighttime surface temperature increased by 18 K (Smith 2004).
- These observations are consistent with models and theories that suggest that reflection of longwave radiation by aerosols aloft will cause the surface to cool during the day, while at night, IR radiation emitted from the atmosphere in all directions will increase surface temperature (Haberle *et al.* 1982, 1999).
- Following the storm, both daytime surface and atmospheric temperatures decreased for a period of one Martian year compared to year before the storm, while nighttime surface and atmospheric temperatures remained almost unchanged (Smith 2004).
- Smith reports a decrease in global surface temperature of 3K and attributes these observations to increased albedo following the storm, which increases reflection of solar radiation and decreases absorption at the surface.
- Cantor (2005) calculated a 3% rise in the average surface albedo following the storm.

Discussion

Based on our analysis of these MGS data, we propose the following working hypothesis to explain the dynamical processes responsible for PDS initiation and expansion. Six eastward-traveling transient baroclinic eddies triggered the MY 25 precursor storms in Hellas during L_s=176.2–184.6^{o} due to the enhanced dust lifting associated with their low-level wind and stress fields.

This was followed by a seventh eddy that contributed to expansion on L_s=186.3^{o}. Increased opacity and temperatures from dust lifting associated with the first three eddies enhanced thermal tides which supported further storm initiation and expansion out of Hellas.

Constructive interference of eddies and other circulation components including sublimation flow, anabatic winds (daytime upslope), and diurnal tides may have contributed to storm onset in and expansion out of Hellas.

References

Flammarion, C., 1892: *La planéte Mars et ses conditions d'habitabilité: Synthèse générale de toutes le observations*. Vol. I, Gauthier-Villars et Fils, Imprimeurs-Libraires de l'observatoire de Paris.

Haberle, R. M., 2003: Planetary Atmospheres: Mars. Encyclopedia of Atmospheric Sciences, J. R. Holton, J. A. Curry, and J. A. Pyle, Eds., Academic Press, 1745–1755.

Haberle, R. M., 1997: Mars: Atmosphere. Encyclopedia of Planetary Sciences, J. H. Shirley, and R. W. Fairbridge, Eds., Springer, 432–440.

Leovy, C., 2001: Weather and climate on Mars. *Nature*, **412**, 245–249.

Noble, J., *et al.,* 2011: Comparison of TES FFSM Eddies and MOC Storms, MY 24–26. *Mars Atmosphere Workshop 4*, Paris, France.

Owen, T., 1992: The Composition and Early History of the Atmosphere of Mars. Mars, H. H. Kieffer, B. M. Jakosky, C. W. Snyder, and M. S. Matthews, Eds., University of Arizona Press, 818–834.

Read, P. L., and S. R. Lewis, 2004: The Martian climate revisited: atmosphere and environment of a desert planet. Springer-Praxis Books, 326 pp.

Smith, M. *et al.,* 2000: Mars Global Surveyor Thermal Emission Spectrometer (TES) observations of dust opacity during aerobraking and science phasing. *Journal of Geophysical Research*, **105**, 9539–9552.

Wilson, R. J., R. M. Haberle, J. Noble, e*t al*., 2008: Simulation of the 2001 Planet-encircling Dust Storm with the NASA/NOAA Mars General Circulation Model. *Mars Atmosphere Workshop 3,* Williamsburg, VA.

Wilson, R. J., J. Noble, and S. J. Greybush, 2011: The derivation of atmospheric opacity from surface temperature observations. *Mars Atmosphere Workshop 4,* Paris, France.

Zurek, R. W., J. R. Barnes, R. M. Haberle, and J. B. Pollack, 1992: Dynamics of the atmosphere of Mars. Mars, H. H. Kieffer, *et al.,* Eds., University of Arizona Press, 835–933.